Lead Compensator Design for Single-Phase Quasi Z-Source Inverter

Sut Khan Yong[1], Kah Haw Law[1], Wendy Pei Qin Ng[1] and Mohamed Dahidah[2]
[1]*Curtin University, Miri, CDT 250 98009 Malaysia.*
[2]*School of Electrical and Electronic Engineering, Newcastle University, Newcastle upon Tyne, UK.*
sutkhan.yong@postgrad.curtin.edu.my

***Abstract*—This paper presents a new control method for single-phase quasi-Z-source inverter (qZSI). At present, trial and error, as well as tuning of traditional proportional integral (PI) controller techniques, are utilized at the aforementioned topology to achieve system stability. Nevertheless, drawbacks of PI controlled based converter/inverter topologies are realized which include slow response speed and poor robust performance compared with the systems uncertainties and exogenous disturbances. In this work, lead compensator in control of the unipolar sinusoidal pulse width modulation (SPWM) qZSI is demonstrated to show its superiority against traditional PI control based on the derived qZSI's small signal model. The methods to obtain the controllers' parameters of the lead compensator is also documented in this paper. The effectiveness and the theoretical analysis of the proposed approach are verified through simulation studies for different loading conditions. The simulation demonstrates the correctness and effectiveness of the proposed control method in providing fast dynamic and transient response through frequency response analysis.**

***Index Terms*—Quasi-Z-Source Inverter; Lead Compensator; Pulse Width Modulation; Controller; Transient Response.**

I. INTRODUCTION

Nowadays, renewable energy source such as solar and wind energy are commonly being used to replace fossil fuel and crude oil. With the increasingly favoured in the application of photovoltaic (PV) systems, power electronics have been extensively utilized onto inverter implementation, particularly for flexible alternating current transmission systems (FACTS) devices. However, power quality, efficiency, and reliability are still the main issues that need to take note of from the aforementioned applications. Typically, excessive reactive power is one of the significant threats to power system security and stability that causes increase of power loses in electrical transmission. Therefore, static synchronous compensator (STATCOM), one of the shunt connected FACTS devices, is commonly employed to provide reactive power compensation. Traditional two-stage inverter formed by voltage source inverter (VSI) or current source inverter (CSI) linked with a DC-DC buck/boost/flyback converter has drawbacks. This includes high cost, low efficiency, and complex control. In addition, traditional inverter is vulnerable to the electromagnetic interference noise. Furthermore, the series connected power switches of each phase leg cannot be gated on simultaneously as to prevent shoot-through or short circuit from happening.

The existing ZSI and qZSI shown in Figure 1 has recently been replacing traditional inverter topologies due to its capability of gating on both of the series connected power switches at the same time. Specially, qZSI is an improved version of ZSI due to its ability to draw continuous current from the input source [1]-[2]. Besides that, qZSI has significant operational efficiency and reliability improvement as well as the odd-order harmonic components reduction from the generated output voltage waveform. In addition, qZSI network can perform voltage boosting and inversion in a single stage topology. Furthermore, qZSI allows discontinuous conduction mode (DCM) operation where the input current falls to zero during some part of the switching period [2].

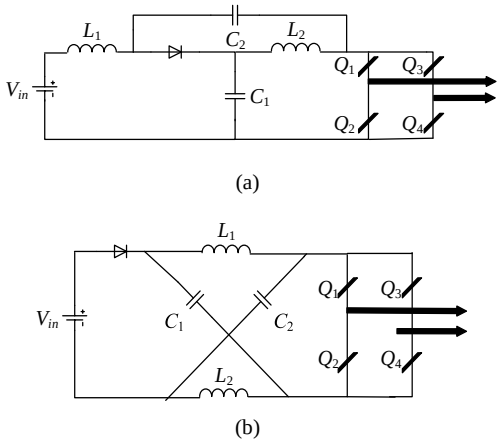

Figure 1: Single-phase (a) qZSI and (b) ZSI.

PI controller has been widely used in many control applications due to its structural simplicity and the ability to solve practical control problems. However, PI controller employed in converter/inverter topologies shows some drawbacks, which include slow response speed as well as poor robust performance against the systems' uncertainties and exogenous disturbances. Moreover, the controller's parameters of the PI controller are not specifically defined [3]-[4] and the method to obtain the controller's parameters is not discussed [5]. Also, there are several existing works revealing that the use of PI controller will lead to poor transient and dynamic responses as well as causing instability of the system due to different variations of parameters and operating points in the system [6]-[7]. For instance, H2/H∞ based optimal controller is proposed in [8] to improve transient and steady-state performances in grid-connected converters. From the simulation results, the proposed controller demonstrates better performance in tracking the changing of the reference currents of the AC and DC-link voltage distribution. Besides, it offered lower overshoot and attained more promising transient response than PI controller

even though the essential parameters are remain varying. Nevertheless, it cannot evaluate the robustness under exogenous disturbances and system parameter perturbations [8].

The Proportional Resonant (PR) controller is demonstrated in several works as an alternative solution to qZSI control system [9]-[10]. For instance, PR controller, rather than PI controller, is chosen in [9] to control a sinusoidal reference in a voltage restorer system. This is because PR controller can provide high gain value for the selected fundamental frequency and keep other frequencies at low gain value while conversely, the gain of the PI controller is limited by the gain at resonant frequency. In addition, PI controller introduces phase shift to the output voltage while in contrast, PR controller avoids the aforementioned phenomenon and reduces the steady-state error. Nonetheless, the work concludes that PR controller provides promising performance when input error is varying. Furthermore, [10] has demonstrated that PI controller used in the current control loop is unable to remove the low-order current harmonics due to the bandwidth limitation. To counteract it, a higher P gain is needed to increase the bandwidth but with the cost of altering the system stability. Alternatively, it is difficult for a PID controller to achieve good performance when there is a right-hand-plane zero in the system (i.e. non-minimum phase) [11]. Therefore, Type-II compensator was introduced to overcome the problem and ensure robustness of the control system. The working principle of Type-II compensator is to provide classical loop shaping by modifying the gain and phase characteristics of open-loop frequency response [12]. Several works have shown the benefits of using Type-II compensator in current and voltage control system [3]-[4], [12]-[13]. For instance, [13] demonstrated that Type-II compensator is able to reduce the overshoot of the pulse width modulation (PWM) generated output voltage during transient time. A Type-II compensator is a lead compensator with two poles (i.e., one pole at the origin) and one zero. Type-II compensator is essentially a Type-I compensator in series with a lead controller. Type-II compensator can provide 0° to 90° phase boost with zero state error. On the other hand, lead/lag compensator is one of the most commonly used techniques for designing control systems. In [14], phase lead compensator is used to replace the PI controller to control the speed of the machine. Besides, performance comparison between PID controller and lead/lag compensator was investigated in [15]. The results showed major improvement in robot performance even though there was a small increase of the off-line design and tuning effort. However, yet no research has been conducted to develop voltage or current control loop using a lead/lag compensator for qZSI.

This work presented a lead compensator for single-phase qZSI. When compared with the aforementioned controllers, the proposed controller was simple to be implemented. In addition, proposed control strategy could effectively improve both the dynamic performance and transient stability as well as enhance the DC-link voltage stability of qZSI through different loading conditions.

This paper is organized as follows: Section II presents the fundamental operation and modelling of qZSI. Section III addresses the design of the proposed control strategy via small-signal model approach. Selected simulation results are reported in Section IV. Finally, conclusions are summarized in Section V.

II. QZSI Modeling and Operational Principle

The qZSI network is first proposed by Peng in 2008 [1]. Figure 2(a) and 2(b) show the equivalent circuits of shoot through state and non-shoot through state, respectively. The qZSI operates in three different modes (i.e. active state, null state and shoot through state).

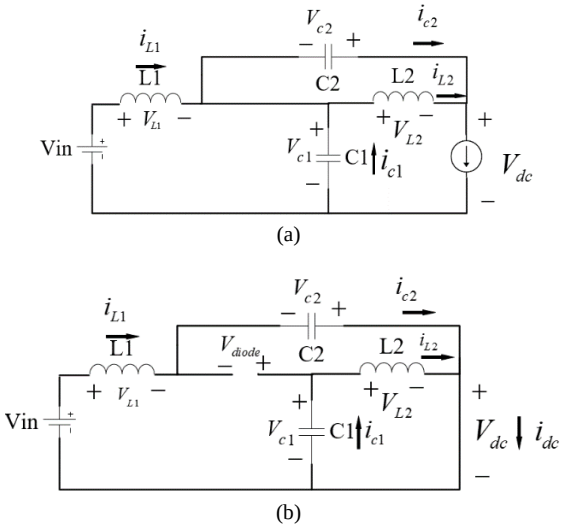

Figure 2: Equivalent circuit of qZSI (a) Non-shoot through state (b) Shoot through state

By rearranging the circuit in Figure 2(a) and 2(b) for better view and understanding, the shoot through state and null state is redrawn and shown in Figure 3(a) and 3(b) respectively.

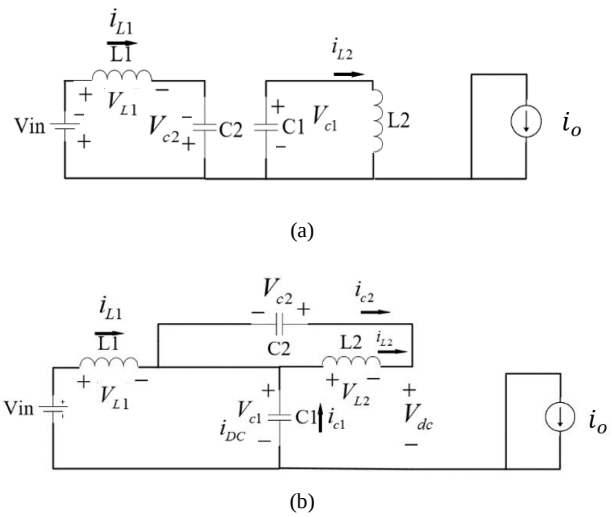

Figure 3: Equivalent operation modes for qZSI (a) shoot through state (b) null state

Particularly, during the shoot through state as depicted in Figure 3(a), either one or two-phase leg of the inverter are being short-circuited to form two active loops. Specifically, one complete loop is attained through the input voltage, V_{in}, capacitor C_2 and inductor L_1 to charge up L_1 while the other loop is through capacitor C_1 and inductor L_2 to charge L_2. Meanwhile, during the non-shoot through state when high-side and low-side switches in the same phase leg are being switched on simultaneously, the diode forward biased. In active state, boosting mechanism occurs while qZSI works as a conventional VSI without employing any dead time; discharging the capacitor C_1 voltage through the inductor L_2

and providing more current to flow through the output load. The null state shown in Figure 3(b) happens when the top or bottom two IGBT switches are turned on simultaneously. During this state, the H-bridge inverter is disconnected from the qZSI impedance network; causing the current flows through inductor L_2 to recharge capacitor C_2 while the current flows through inductor L_1 to charge capacitor C_1 concurrently.

During the shoot-through state, the state space equations of qZSI in steady state can be written in the form of $F\dot{x} = A_1 x + B_1 u$.

$$\begin{bmatrix} L_1 & 0 & 0 & 0 \\ 0 & L_2 & 0 & 0 \\ 0 & 0 & C_1 & 0 \\ 0 & 0 & 0 & C_2 \end{bmatrix} \begin{bmatrix} \dot{i}_{L1}(t) \\ \dot{i}_{L2}(t) \\ \dot{v}_{C1}(t) \\ \dot{v}_{C2}(t) \end{bmatrix} = \begin{bmatrix} 0 & 0 & 0 & 1 \\ 0 & 0 & 1 & 0 \\ 0 & -1 & 0 & 0 \\ -1 & 0 & 0 & 0 \end{bmatrix} \begin{bmatrix} i_{L1}(t) \\ i_{L2}(t) \\ v_{C1}(t) \\ v_{C2}(t) \end{bmatrix} + \begin{bmatrix} 1 & 0 \\ 0 & 0 \\ 0 & 0 \\ 0 & 0 \end{bmatrix} \begin{bmatrix} v_{in}(t) \\ i_o(t) \end{bmatrix} \quad (1)$$

The state equation of non-shoot through state in steady state of qZSI is given as:

$$\begin{bmatrix} L_1 & 0 & 0 & 0 \\ 0 & L_2 & 0 & 0 \\ 0 & 0 & C_1 & 0 \\ 0 & 0 & 0 & C_2 \end{bmatrix} \begin{bmatrix} \dot{i}_{L1}(t) \\ \dot{i}_{L2}(t) \\ \dot{v}_{C1}(t) \\ \dot{v}_{C2}(t) \end{bmatrix} = \begin{bmatrix} 0 & 0 & -1 & 0 \\ 0 & 0 & 0 & -1 \\ 1 & 0 & 0 & 0 \\ 0 & 1 & 0 & 0 \end{bmatrix} \begin{bmatrix} i_{L1}(t) \\ i_{L2}(t) \\ v_{C1}(t) \\ v_{C2}(t) \end{bmatrix} + \begin{bmatrix} 1 & 0 \\ 0 & 0 \\ 0 & -1 \\ 0 & -1 \end{bmatrix} \begin{bmatrix} v_{in}(t) \\ i_o(t) \end{bmatrix} \quad (2)$$

The average values of the capacitor voltages V_{C1} and V_{C2} are defined as:

$$V_{C1} = \frac{1 - D_o}{1 - 2D_o} V_{in} \quad (3)$$

$$V_{C2} = \frac{D_o}{1 - 2D_o} V_{in} \quad (4)$$

The average value of DC-link voltage V_{dc} can be written as:

$$V_{DC} = \frac{1}{1 - 2D_o} V_{in} = BV_{in} \quad (5)$$

where D_o in (6) defines the steady-state shoot-through duty cycle and B in (7) is the boost factor resulting from the shoot-through state which can be derived as:

$$D_o = \frac{V_{C1} - V_{in}}{2V_{C1} - V_{in}} \quad (6)$$

$$B = \frac{1}{1 - 2D_o} \quad (7)$$

III. Control Strategy of PWM Shoot Through Duty Ratio

Lead compensation can effectively reduce the overshoot percentage and increase the gain crossover frequency of a system in order to realize fast transient response. On the other hand, reduction of overshoot percentage can also be attained by increasing the phase stability margin at the crossover frequency. Figure 4 illustrates the proposed voltage-current closed-loop control system that generates the shoot-through duty ratio to acquire the desire buck and boost capabilities of qZSI. It is designed based on qZSI small signal equivalent circuit. To achieve DC-link voltage control, the difference between the DC-link voltage reference value, $V_{dc}{}^*$ and the actual measured DC-link voltage, V_{dc} will pass through a lead compensator $G_c(s)$ and generate a corresponding shoot-through duty ratio d towards the unipolar sinusoidal PWM technique.

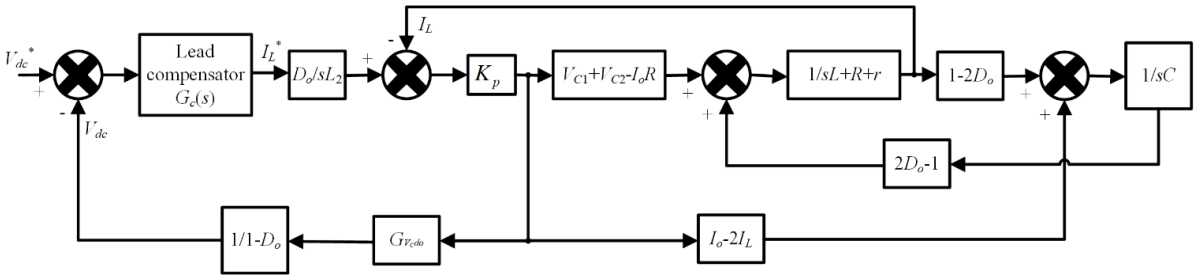

Figure 4: Voltage-current closed loop control strategy

The transfer function of the DC-link voltage to the inductor current is derived as:

$$G_{\widehat{I_L}\widehat{V_{dc}}} = \left(\frac{D_o}{L}\right)\left(\frac{1}{s}\right) \quad (8)$$

Equation (8) indicates that the transfer function consists of a pure integral multiply with a constant, which correspond to the integral term of PI controller and type II error amplifier. The transfer function of the DC capacitor voltage against the shoot-through duty cycle is derived as:

$$G_{\widehat{v_c}\hat{d}} = \frac{\widehat{v_c}(s)}{\hat{d}(s)} = \frac{(I_o - I_{L1} - I_{L2})\big(Ls + (r + R)\big) + (V_{C1} + V_{C2} - RI_o)}{(LCs^2 + C(r + R)s + (1 - 2D_o)^2)} \quad (9)$$

The open loop transfer function of the current inner loop is defined as:

$$G_{\widehat{I_L}\hat{d}} = \frac{\widehat{I_L}(s)}{\hat{d}(s)} = \frac{(1 - 2D_o)(I_o - 2I_L)(Ls + R + r)}{(Ls + R + r)[(LCs^2 + (R + r)Cs) + (1 - 2D_o^2)]} + \frac{(V_{c1} + V_{c2} - I_oR)(LCs^2 + (R + r)Cs)}{(Ls + R + r)[(LCs^2 + (R + r)Cs) + (1 - 2D_o^2)]} \quad (10)$$

where I_{L1} and I_{L2} are the currents flow through inductor L_1 and L_2, respectively, I_o is the DC-link current, R is the equivalent series resistance of a capacitor, r is the equivalent series resistance of an inductor, while V_{C1} and V_{C2} are the voltage of capacitor C_1 and C_2, respectively.

The lead compensator general equation is defined as:

$$G_c(s) = \frac{\frac{1}{\gamma}\left(s+\frac{1}{T}\right)}{s+\frac{1}{\gamma T}} \quad (11)$$

The following summarizes are the sequences to obtain all the parameters in (11):

Step 1: Determine the system type of a unity feedback system to calculate the steady-state error from its closed-loop or the open-loop transfer function.

Step 2: Determine the closed loop bandwidth to meet settling time and peak time requirement. By setting the desired overshoot percentage, the damping ratio of the system is calculated by:

$$\xi = \frac{-\ln\left(\frac{\%OS}{100}\right)}{\sqrt{\pi^2 + \ln^2\left(\frac{\%OS}{100}\right)}} \quad (12)$$

where ξ is the damping ratio and *%OS* is the overshoot percentage of the uncompensated system.

The bandwidth of the system is defined as:

$$\omega_{BW} = \frac{\pi}{T_p\sqrt{1-\xi^2}}\sqrt{(1-2\xi^2)+\sqrt{4\xi^4-4\xi^2+2}} \quad (13)$$

where T_p is the peak time of the uncompensated system.

Step 3: Increase the low-frequency magnitude responses to reduce the steady-state error. In other words, the gain *K* should be varied to attain the desired steady-state error.

Step 4: Plot a bode plot and determine the uncompensated system's phase margin.

Step 5: Choose the phase margin which is able to meet the required damping ratio and overshoot percentage via (16) as follows:

$$\emptyset_{PM} = \tan^{-1}\frac{2\xi}{\sqrt{-2\xi^2+\sqrt{1+4\xi^4}}} \quad (14)$$

Step 6: Calculate the desired phase contribution of the lead compensator by adding a correction factor to compensate for the lower uncompensated system's phase angle.

Step 7: Determine γ from the lead compensator's required phase contribution and determine the magnitude of the compensator at the peak of the phase curve. γ can be determined using equation as follow:

$$\gamma = \frac{1-\sin\emptyset_{max}}{1+\sin\emptyset_{max}} \quad (15)$$

where Φ_{max} is the total phase contribution required from the compensator.

The magnitude of the compensator is derived as:

$$|G_c(j\omega_{max})| = \frac{1}{\sqrt{\gamma}} \quad (16)$$

The phase margin frequency, ω_{max} can be determined by selecting the frequency at which the uncompensated system's magnitude is the negative of the magnitude of the compensator where the magnitude is in logarithm scale.

Step 9: Determine the value *T* of the compensator.

$$T = \frac{1}{w_{max}\sqrt{\gamma}} \quad (17)$$

Step 10: Redesign of the compensator by repeating the procedure using different correction factor if the requirement is not met.

Table 1 has summarized the desired transient parameter used to design the lead compensator.

Table 1
Desired Transient Parameter

Parameters	Value
%Overshoot	5%
Peak time, T_p	0.05s
Required phase margin	64.63°
Damping ratio	0.6901

IV. Simulation Results

Intensive simulation works had been performed using MATLAB/SIMULINK for the proposed qZSI and its associated control scheme. The proposed lead controller maintaining a constant DC-link voltage of 240V from an input DC voltage source of 24V under different AC loading conditions (i.e., resistive load A=34Ω and B=70Ω, respectively). The parameters selected for qZSI impedance network are C_1=C_2=68mF and L_1=L_2=1.2μF. The switching frequency used in the simulation is 10kHz. The desired overshoot percentage value (i.e., %*OS*) used to design the compensator is 5%.

Table 2 shows the controller parameters values for both lead compensator and PI controller used in this work. The parameter of the PI control in the voltage control loop and P controller in the inner current loop are obtained by tuning the response speed for P controller and both response speed and transient behavior for PI controller. The P gain of current inner loop for both lead and PI controller control system are fixed to $4.621x10^{-5}$.

Table 2
Controller parameters (Lead Compensator and PI controller)

Lead compensator		PI Controller ($P + I\left(\frac{1}{s}\right)$)	
Gain	5.06	Proportional gain (P)	38.71
Transfer function $G_c(s)$	$5.06*\left(\frac{s+16054.7}{s+81172.9}\right)$	Integral coefficient (I)	2943.35

Figure 5 depicts the relationship between the DC-link reference V_{dc}^* and V_{dc}.

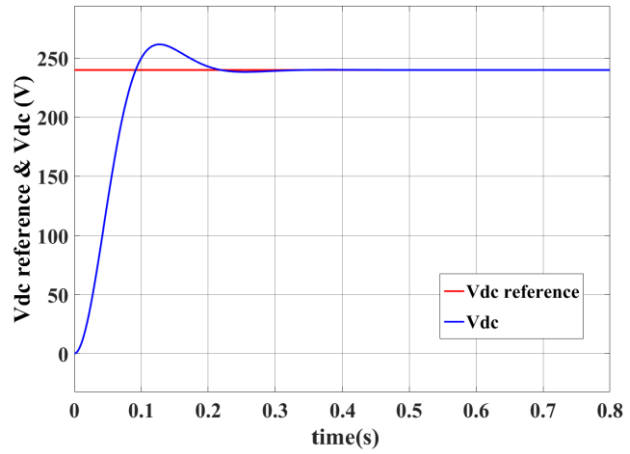

(a)

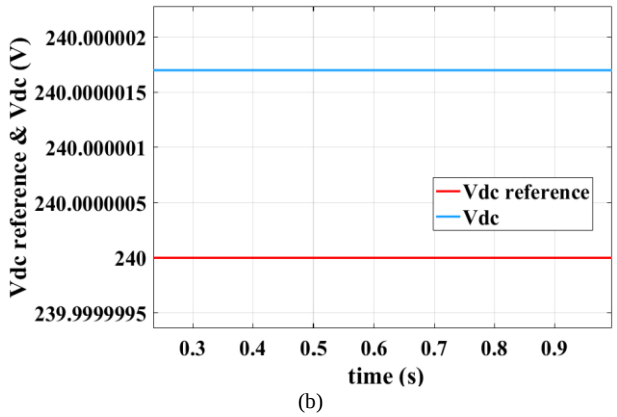

(b)

Figure 5: Relationship between DC-link (a) V_{dc}^{*} and measured V_{dc}, and (b) steady-state error from the proposed mathematical model

When compared with the preset desired %*OS*, it is concluded from Figure 5(a) that an acceptable resultant %*OS* of 9.04% (i.e., accounted for an approximate peak value of 261.7V) is attained. Fast transient response is also realized in Figure 5(a), measuring from the peak and settling time of 0.127s and 0.345s, respectively. Figure 5(b) illustrates a satisfactory steady-state error value of lower than 2μV.

Figure 6 illustrates the measured qZSI DC-link voltage V_{dc} to inhibit external disturbances. It is noted that the AC load is changed from load A to B at 1s.

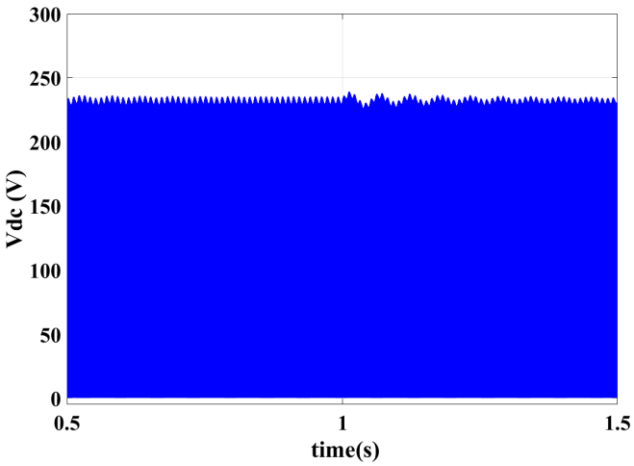

Figure 6: QZSI DC-link voltage, V_{dc}

Figure 7 shows the frequency response of the original system and the compensated system. From the bode plot, the phase margin of the uncompensated system is measured to be 0.84°. However, after the system has been compensate by using a lead compensator, the phase margin of the system can be improved and increased to 63.3°. This phase margin improvement reduces the overshoot percentage, which is corresponding to the desired phase margin calculated during the design of the lead compensator. However, the gain crossover frequency has been greatly reduced, which in turn, slows down the transient response. Despite, from Figure 5(a) the peak time and the settling time obtained from the system is still encouraging. The reduction of the gain crossover frequency might due to the gain of the P controller in the inner current loop, which is incredibly small. Nevertheless, Figure 6 concluded that with the proposed control scheme, DC-link voltage can be kept invariable even the load changes.

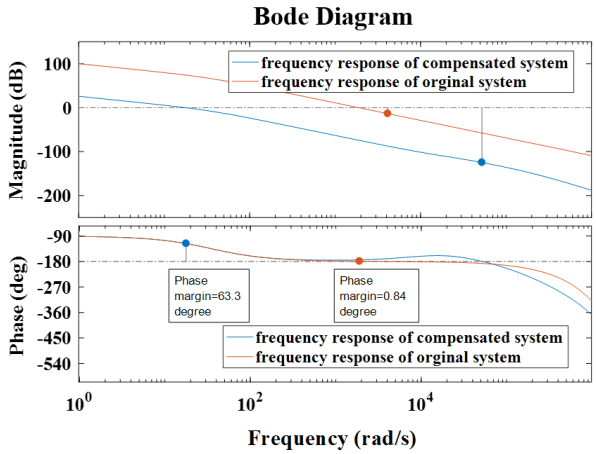

Figure 7: Bode plot

Similar observation from Figure 6 is realized in Figure 8 for the actual voltages measured across capacitor C_1 and C_2.

Figure 9 illustrates the measured inductor current when lead controller and PI controller were used. From the graph, it is obvious that the overshoot of the inductor current is high when PI controller is used. The maximum inductor current jump up to 100A which will eventually damage the experimental circuit. However, this issue can be resolve by using AC load with higher resistance to limit the inductor current. Nevertheless, when a lead compensator is used, the inductor current only spike until a maximum amount of 25.2A which is acceptable to be conducted in an experimental prototype.

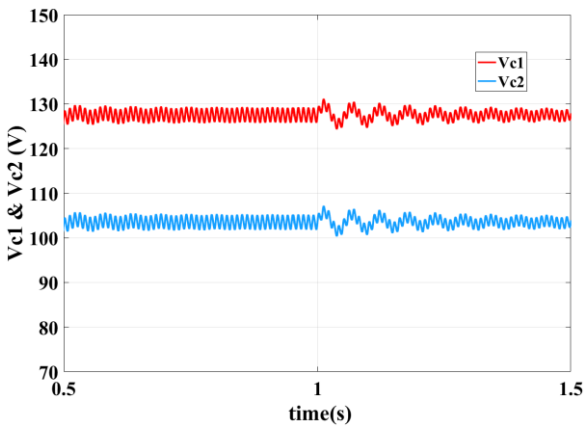

Figure 8: QZSI capacitor voltages: V_{C1} & V_{C2}

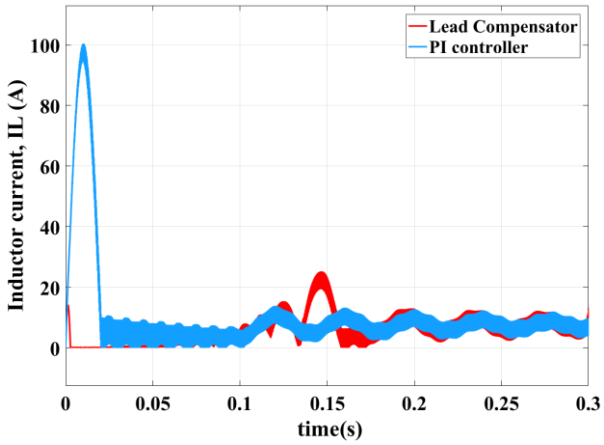

Figure 9: Comparison between inductor current I_{L1} of QZSI using Lead Compensator and PI controller

V. Conclusion

In this paper, the small signal model of qZSI has been derived and analyzed. A lead compensator has been designed to improve the dynamic performance as well as the transient response of the qZSI via frequency response analysis. From the simulation results, it is concluded that the compensator is robust at which the design has fulfilled the requirement of the desired frequency and transient response of the system. Moreover, the proposed controller was able to achieve zero tracking error. The proposed control strategy cultivates remarkable method to enhance the DC-link voltage stability through different loading conditions. Also, the proposed control method is simple to implement.

Acknowledgement

Immense gratitude to Dr. Law Kah Haw for guiding and advising me throughout this project. This work was supported by the Ministry of Higher Education Malaysia under the Fundamental Research Grant Scheme Project No. FRGS/1/2016/TK07/CURTIN/03/02.

References

[1] S. Andrews and S. Joshi, "Performance Improvement of Dynamic Voltage Restorer using Proportional - Resonant Controller," in Proceedings of PCIM Europe 2015; International Exhibition and Conference for Power Electronics, Intelligent Motion, Renewable Energy and Energy Management, 2015, pp. 1-8.

[2] B. Ge, F. Z. Peng, H. Abu-Rub, F. J. T. E. Ferreira, and A. T. d. Almeida, "Novel Energy Stored Single-Stage Photovoltaic Power System With Constant DC-Link Peak Voltage," IEEE Transactions on Sustainable Energy, vol. 5, pp. 28-36, 2014.

[3] L. K. Haw, M. S. A. Dahidah, and H. A. F. Almurib, "A New Reactive Current Reference Algorithm for the STATCOM System Based on Cascaded Multilevel Inverters," IEEE Transactions on Power Electronics, vol. 30, pp. 3577-3588, 2015.

[4] L. Kah Haw, M. S. A. Dahidah, G. S. Konstantinou, and V. G. Agelidis, "SHE-PWM cascaded multilevel converter with adjustable DC sources control for STATCOM applications," in Proceedings of The 7th International Power Electronics and Motion Control Conference, 2012, pp. 330-334.

[5] Z. Li, C. Zang, P. Zeng, H. Yu, H. Li, L. Gao, et al., "Robust mixed H2 / H∞ based optimal controller design for single-phase grid-connected converter," in 2016 Chinese Control and Decision Conference (CCDC), 2016, pp. 1230-1234.

[6] Y. Liu, B. Ge, F. J. T. E. Ferreira, A. T. d. Almeida, and H. Abu-Rub, "Modeling and SVPWM control of quasi-Z-source inverter," in 11th International Conference on Electrical Power Quality and Utilisation, 2011, pp. 1-7.

[7] M. Mosa, R. S. Balog, and H. Abu-Rub, "High-Performance Predictive Control of Quasi-Impedance Source Inverter," IEEE Transactions on Power Electronics, vol. 32, pp. 3251-3262, 2017.

[8] D. Sun, B. Ge, X. Yan, H. Abu-Rub, D. Bi, and F. Z. Peng, "Impedance design of quasi-Z source network to limit double fundamental frequency voltage and current ripples in single-phase quasi-Z source inverter," in 2013 IEEE Energy Conversion Congress and Exposition, 2013, pp. 2745-2750.

[9] D. Vinnikov, I. Roasto, R. Strzelecki, and M. Adamowicz, "CCM and DCM operation analysis of cascaded quasi-Z-source inverter," in 2011 IEEE International Symposium on Industrial Electronics, 2011, pp. 159-164.

[10] F. B. Remus Teodorescu, Marco Liserre, "Proportional-Resonant Controllers. A New Breed of Controllers Suitable for Grid-Connected Voltage-Source Converters," Journal of Electrical Engineering, pp. 1-4.

[11] K. Yu, F. L. Luo, and M. Zhu, "Study of an improved Z-source inverter: Small signal analysis," in 2010 5th IEEE Conference on Industrial Electronics and Applications, 2010, pp. 2169-2174.

[12] A. Ghosh and S. Banerjee, "Design and implementation of Type-II compensator in DC-DC switch-mode step-up power supply," in Proceedings of the 2015 Third International Conference on Computer, Communication, Control and Information Technology (C3IT), 2015, pp. 1-5.

[13] M. N. S. K. Shabbir, E. Haque, and A. B. Shams, "Reduction of settling time and minimization of transient overshoot of a buck converter," in 2016 5th International Conference on Informatics, Electronics and Vision (ICIEV), 2016, pp. 345-350.

[14] B. Nayak, S. Kumar, and S. S. Dash, "Design of phase lead compensator for buck converter fed adjustable speed drive," in 2015 Communication, Control and Intelligent Systems (CCIS), 2015, pp. 304-308.

[15] Y. Chen, "Replacing a PID controller by a lat-lead compensator for a robot-a frequency-response approach," IEEE Transactions on Robotics and Automation, vol. 5, pp. 174-182, 1989.